710361

Research in Automobile Dynamics - A Computer Simulation of General Three-Dimensional Motions

Raymond R. McHenry
Transportation Research Dept., Cornell Aeronautical Laboratory, Inc.

DURING THE PAST FOUR YEARS the Cornell Aeronautical Laboratory, Inc. (CAL) has developed several versions of a computer simulation of general, three-dimensional automobile dynamics (Fig. 1), for study of accident-related maneuvers on irregular terrain. This research has been performed under sponsorship of the Traffic Systems Div. of the Bureau of Public Roads (BPR),* as a part of an overall research program entitled "Single Vehicle Accident Minimization, Rural Highways."

The initial version of the BPR-CAL computer simulation (1-3)** is aimed at general applications to roadside design problems, including collisions. The emphasis on prediction of responses to collision forces that act directly on the sprung mass is reflected in the use of a number of deliberate simplifications in the analytical treatment of vehicle details related to handling characteristics. However, despite the simplifications, a high degree of correlation has been achieved between predicted and experimental responses in a rigorous investigation of validity that included both separate and combined cornering and ride motions (1-3), (Figs. 2 and 3). An earlier series of gross comparisons of response predictions, with test results from the literature which included a broader spectrum of violent maneuvers as well as collisions, has also indicated generally accurate predictions, within the limitations of the fragmentary data available for vehicle parameters and measured responses (4, 5).

As a supplement to the conventional time-history form of simulation outputs, an auxiliary computer-graphics program has also been developed within the CAL research program (6, 7) to produce perspective drawings of the simulated vehicle as seen from selected viewing positions and at selected times during a predicted event (for example, Fig. 4).

*The reported research was performed under Contract No. CPR-11-3988. The opinions, findings, and conclusions expressed in this paper are those of the author and not necessarily those of the Bureau of Public Roads.

**Numbers in parentheses designate References at end of paper.

ABSTRACT

A digital computer simulation of complex, three-dimensional dynamics of automobiles on irregular terrain is described which is suitable for studies related to vehicle braking systems and to the driving task, including the upper limits of control as well as the linear ranges of operation. The reported simulation is an extended version of an earlier, validated mathematical model. A number of refinements and extensions of the analytical treatments of tire forces, suspension properties, and terrain definitions, have been incorporated. Also, analytical representations of the braking system and driveline, and approximations of rolling resistance and aerodynamic drag, have been introduced. Sample outputs of the modified computer program are presented and discussed.

The initial version of the simulation program (described in detail in Refs. 1 and 2), which was programmed for a digital computer in the Fortran IV language for ease of transfer, has been distributed by BPR to a total of twenty-three research organizations, to date.

Subsequent to the completion of the cited validation study (1-3) with the initial version of the computer simulation, further development efforts have been applied to three separate versions, each aimed at a different aspect of the single vehicle accident problem. In particular, the initial "collision" version is currently being modified to incorporate an improved subroutine for treatment of collision forces, and two "non-collision" versions have been separately developed. The first of the "noncollision" versions, which has been applied in studies of vehicle dynamics and of the driving task (8, 9), includes a more realistic simulation of the suspension bumpers

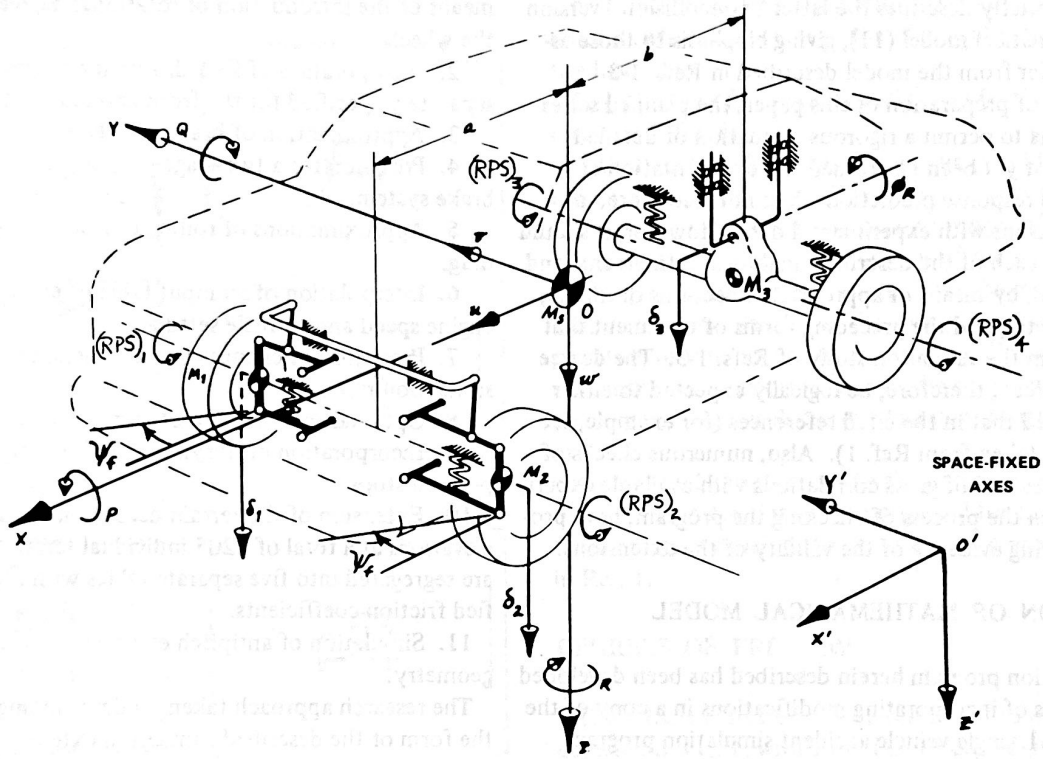

Fig. 1 - Analytical representation of vehicle

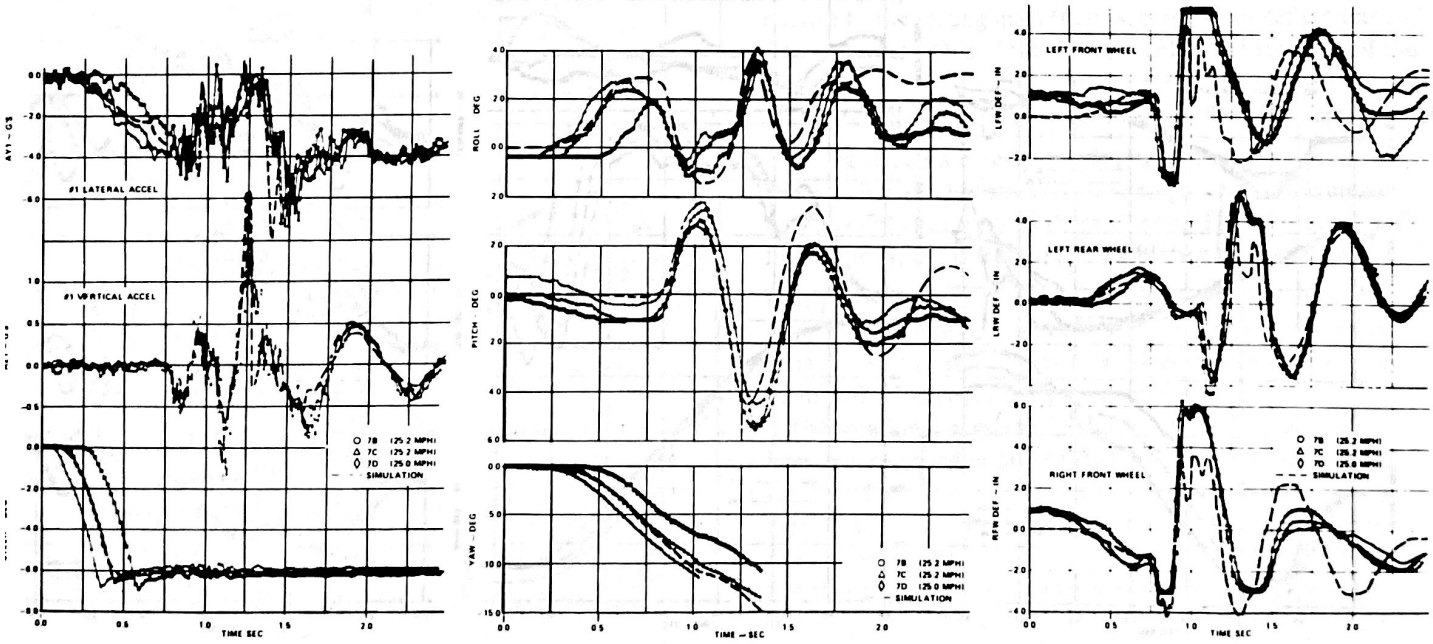

Fig. 2 - Measured and simulated responses of vehicle traversing 7.1 deg, 6.75 in. high ramp while cornering at 0.4 g

and an extended capability for terrain definition, but it retains the "friction circle" concept for treatment of combined circumferential and side tire forces (1, 10). The second "noncollision" version, which is the primary topic of the present paper, also includes the rotational degrees of freedom of the wheels to permit the use of a "friction ellipse" concept for the tire forces in detailed studies of vehicle dynamics at the upper limits of control.

This paper briefly describes the latter "noncollision" version of the mathematical model (11), giving emphasis to those aspects that differ from the model described in Refs. 1-3.

At the time of preparation of this paper, the planned series of experiments to permit a rigorous evaluation of detailed validity has not yet been performed. The presentation of representative response predictions does not, therefore, include comparisons with experimental data. However, it should be noted that each of the described analytical refinements and extensions can, by means of appropriate selections of inputs, be suppressed to yield the preceding forms of treatment that were applied in the validation study of Refs. 1-3. The degree of correlation can, therefore, be logically expected to either equal or exceed that in the cited references (for example, see Figs. 2 and 3, taken from Ref. 1). Also, numerous checks of energy balances and of gross correlations with available experimental data, in the process of checking the program, have provided convincing evidence of the validity of the extensions.

DESCRIPTION OF MATHEMATICAL MODEL

The simulation program herein described has been developed by the process of incorporating modifications in a copy of the basic BPR-CAL single vehicle accident simulation program (1) in which the subroutines related to sprung mass impact were removed and the corresponding core storage was, thereby, made available for new subroutines related to nonimpact dynamics (for example, braking system and driveline details, expanded terrain tables, refinements in suspension details, etc.). In particular, the following extensions or refinements of analytical features are included in the modified computer simulation:

1. Implementation of a "friction ellipse" concept, by means of the introduction of rotational degrees of freedom at the wheels.
2. Incorporation of four different options in brake type, separately specified for the front and rear of the vehicle.
3. Approximation of brake fade effects.
4. Provision for a two-stage proportioning valve in the brake system.
5. Approximations of rolling resistance and aerodynamic drag.
6. Interpolation of an input table of engine torque versus engine speed and throttle setting.
7. Provision for changes in transmission ratio during a simulation run.
8. Optional specification of rear or front drive.
9. Incorporation of unsymmetrical, energy-dissipating suspension stops.
10. Extension of the terrain definition to include detailed elevations at a total of 2205 individual terrain points, which are segregated into five separate tables with separately specified friction coefficients.
11. Simulation of antipitch effects (12) of the suspension geometry.

The research approach taken, in determining the extent and the form of the described simulation extensions and refinements, has been that of producing a general and relatively

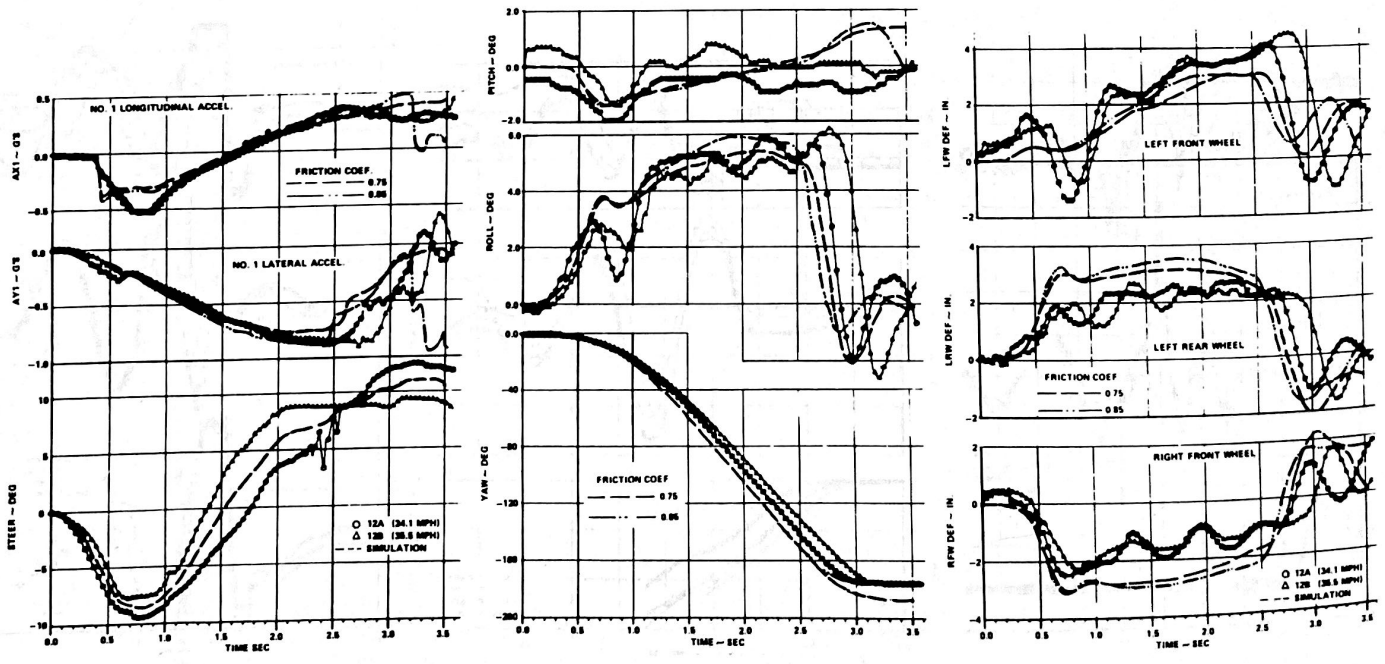

Fig. 3 - Measured and predicted responses of vehicle in forward skid on dry pavement

comprehensive overall representation of the vehicle and its braking system. To a large extent, properties of the braking system and of the tires are defined by means of readily adjustable empirical relationships or tabular inputs, with formats that permit direct application of measured component characteristics, as opposed to derived theoretical relationships. In view of the empirical nature of many aspects of the design of brake systems and tires, this general approach was considered to be preferable to an attempted development of new theoretical analyses of fundamental phenomena within the system. For example, validated predictive relationships are not known to exist for:

1. Drum-brake torque versus brake hydraulic pressure.
2. Brake fade and the frequently attendant redistribution of braking effort.
3. Tire-ground friction versus rotational slip for ranges of vehicle speed, road surface conditions, tire load, and pressure and tread type and condition.
4. Effects of antipitch suspension geometry on the occurrence of wheel lock (that is, the effects of rapid changes in tire loading).
5. Influence of circumferential forces (braking or traction) on tire side forces.

With the selected approach, it will be possible to investigate the sensitivity of the overall vehicle responses to changes in the various functional relationships, over ranges of loading and operating conditions. Those aspects of the system in which further, more fundamental research will be most beneficial can, thereby, be identified. Obviously, without a broad exploration of interactions within the overall system, an early concentration of effort on one of the many fundamental phenomena might well constitute a poor assignment of priorities.

An overall description of the simulation is next presented. More detailed descriptions are provided for those aspects of the simulation which differ from the basic program described in Ref. 1.

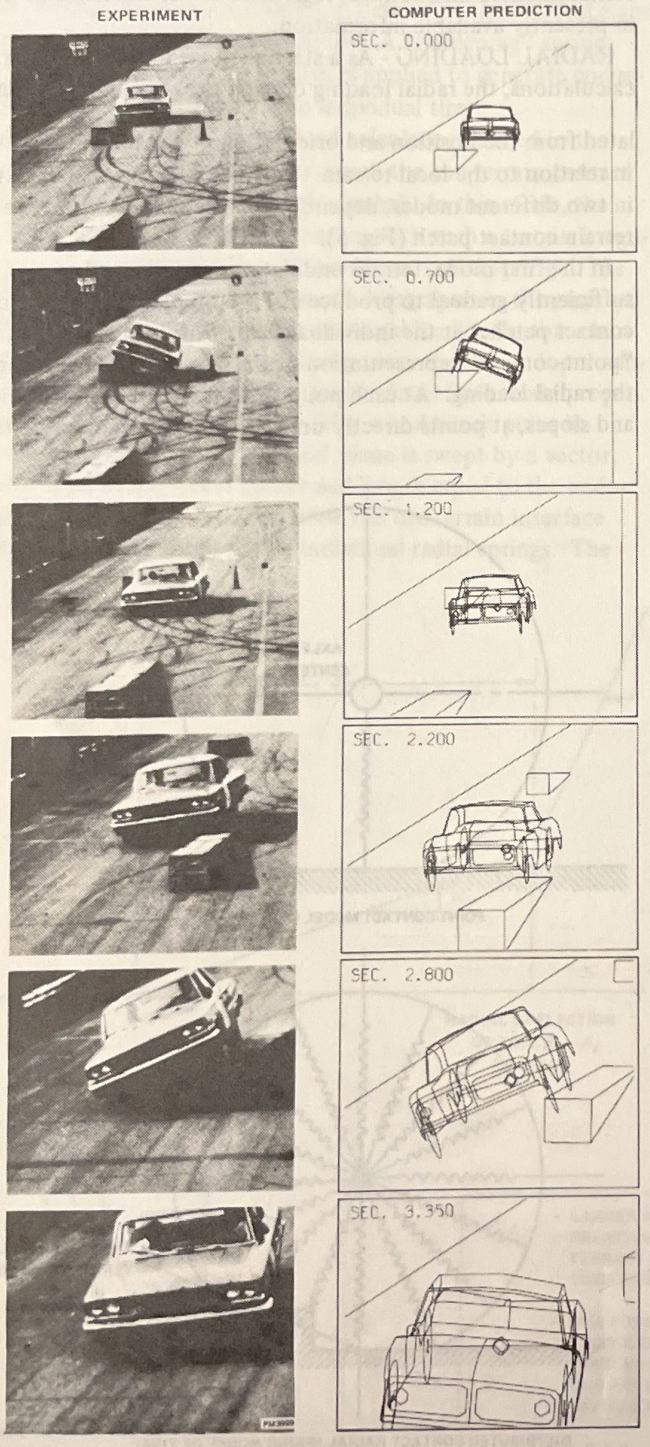

Fig. 4 - Alternate ramp traversal at 30 mph

DEGREES OF FREEDOM

The vehicle is treated as an assembly of four rigid masses, as depicted in Fig. 1, with a total of 15 deg of freedom. These consist of the 6 deg of freedom associated with three-dimensional, rigid-body motions of the sprung mass; a total of 5 deg of freedom associated with motions of the unsprung masses relative to the sprung mass (that is, suspension deflections and front wheel steer); and the 4 rotational deg of freedom of the wheels.

The steer mode degree of freedom, ψ_f, for which any inertial coupling effects are neglected, is introduced at the front wheels when rigid obstacles (for example, curbs) are encountered by either or both of those wheels. The steer angle at the front wheels, ψ_f, is treated as an arbitrary tabular function of time prior to wheel contact with a rigid obstacle. The tabular values at the time of contact and immediately prior to that time are used to provide starting values of angular displacement and velocity for the steer degree of freedom.

The rotational degrees of freedom of the four wheels have been incorporated in order that the effects on tire forces of rotational wheel slip, in braking or traction, can be approximated. It has been assumed that the wheel rotational degrees of freedom are isolated from the existing 11 deg of freedom but that inertial coupling exists between the pair of drive wheels (that is, through the mechanism of the differential gears). Since the differential equations for wheel rotations

can, with this assumption, be isolated from the existing matrix of equations, different time increment sizes are used for the two sets of equations. In this manner, a progressively smaller time increment size is used in the equations defining wheel rotations, as required for solution stability when the spin velocities decrease, while the remainder of the system equations are updated at fixed intervals (for example, every 0.010 sec) throughout a simulation run.

INERTIAL PROPERTIES

Plane OXZ in Fig. 1 is assumed to be a plane of mirror symmetry for the sprung mass.

The c.g. of the front unsprung masses are assumed to coincide with the wheel centers. The front wheels are treated as point masses.

The c.g. of the rear unsprung mass is assumed to coincide with the geometric center of the rear axle. In the treatment of inertial coupling between the sprung mass and the rear unsprung mass, the rear axle is approximated by a thin rod.

Gyroscopic effects of the rotating wheels, drivetrain, and engine, are neglected.

The inertial coupling of rotational motions of the drive wheels, through the differential gears, and the associated effects of driveline inertia are included in the modified simulation.

SUSPENSION GEOMETRY

Camber angles of the individual front wheels relative to the vehicle are determined by interpolation of a tabular input of camber angle as a function of suspension deflection (δ_1 and δ_2 in Fig. 1).

The steer angles of the front wheels relative to the vehicle are assumed to be equal. Roll steer effects in the front suspension are neglected.

Rear axle roll steer is treated as a linear function of the angular degree of freedom of the rear axle, ϕ_R (Fig. 1). Inertial effects are neglected in the steer mode of rear axle motion.

Antipitch effects (12) are approximated by means of coefficients that are entered separately for the front and rear suspensions as tabular functions of the suspension deflections. The product of the wheel torque (braking or traction) at a given wheel and the appropriate antipitch coefficient for that wheel and its suspension deflection is applied as a positive or negative "jacking" effect on the suspension at the given wheel.

TIRE PROPERTIES

The developed simulation of the tires is designed to handle the complete range of tire loading, from a loss of ground contact to conditions of extreme overload. The empirical relationships used to generate the side, braking, and traction forces are aimed primarily at accuracy within the normal ranges of operating conditions. It is assumed that excursions beyond the normal ranges of operating conditions will be of limited duration and that the tire forces, under those conditions, can be treated in a more approximate manner. The selection of this method of approach was also prompted by the dearth of applicable data for tires under the extremes of operating conditions.

One important point should be made before proceeding with the discussion of assumptions regarding tire properties. In a computer program of this sort, provision must be made for all conceivable combinations of operating conditions. The logic and equations of the calculation program must include comprehensive instructions, regardless of the existence of gaps in presently available information.

RADIAL LOADING - As a starting point in the tire force calculations, the radial loading of each tire, F_{R_i}, is first calculated from the position and orientation of the individual wheel in relation to the local terrain. The radial loading is calculated in two different modes, depending on the nature of the tire-terrain contact patch (Fig. 5).

In the first mode, terrain undulations are assumed to be sufficiently gradual to produce essentially planar tire-terrain contact patches at the individual tires. Within this mode, a "point-contact" representation of the tire is used to generate the radial loading. At each point in time, the terrain elevations and slopes, at points directly under each wheel center, are ob-

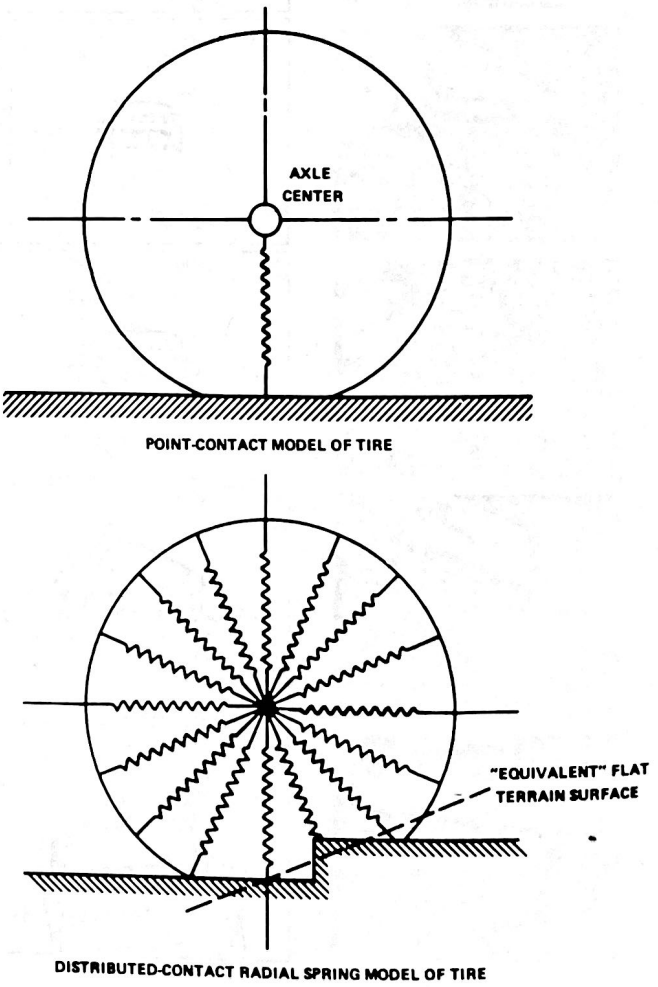

Fig. 5 - Two modes of simulation of radial characteristics of tires

tained either by interpolation of tabular input data for the terrain profile, or, where tables are not used or tabular ranges are exceeded, by treatment of the terrain as a flat, horizontal plane with a zero value of elevation (that is, $Z' = 0$). Determination of the "ground contact points" is accomplished by passing planes through the wheel centers perpendicular both to the wheels and the local ground planes at the individual wheels. At each wheel, the point that lies in all three planes is designated the "ground contact point." The distances between the individual wheel centers and the corresponding "ground contact points" are then calculated to determine the existence and the extent of radial tire deflections. A "hardening" spring characteristic, depicted in Fig. 6, is applied to generate corresponding radial loadings for the individual tires.

The second mode of radial load calculation is used in the case of terrain irregularities for which the tire-terrain contact patch is not planar (for example, curbs). In this mode, the individual wheels that are in contact with such a terrain irregularity are treated as discs with nonlinear radial springs. The radial springs are arbitrarily spaced 4 deg apart in the assumed wheel disc, and they are given identical load-deflection characteristics, which are automatically generated by an input subroutine to match the specified (input data) flat-terrain properties of the point-contact mode (Fig. 6). At each point in time, the lower half of the wheel plane is swept by a vector, with origin at the wheel center and length equal to the undeflected wheel radius, to determine the tire-terrain interface profile at the locations of the individual radial springs. The vector sum of radial forces, corresponding to the deflections and orientations of the individual springs, is used to generate an "equivalent" ground contact point and an "equivalent" flat terrain surface at each wheel, thereby permitting a continuous calculation of approximate side, tractive, and braking forces.

SIDE, BRAKING, AND TRACTION FORCES -

Tire Loading Normal to Ground Contact Patch - The side, braking, and traction forces are, of course, related to the tire load normal to the plane of the tire-terrain contact patch, F'_{R_i}, rather than to the radial tire load, F_{R_i} (Fig. 7). Therefore, it is necessary to find the value of F'_{R_i} corresponding to the radial load, F_{R_i}, and the side force, F_{S_i}. In Fig. 7 the components of the external applied forces, F'_{R_i} and F_{S_i}, along the line of action of the radial tire force, F_{R_i}, are depicted. These force components must be in equilibrium with F_{R_i}, such that

$$F'_{R_i} = F_{R_i} \sec \phi_{CG_i} - F_{S_i} \tan \phi_{CG_i} \qquad (1)$$

Since F'_{R_i} is required for the determination of F_{S_i}, an initial approximation of F_{S_i} is obtained by extrapolation from the previous time increment. Following the calculation of F_{S_i} in

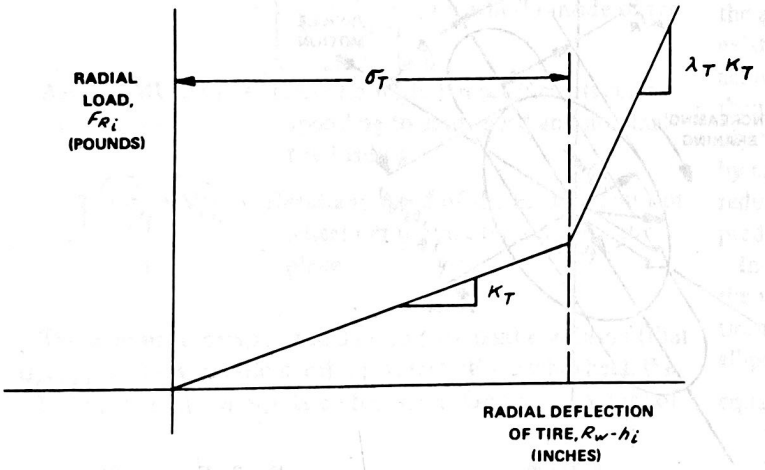

Fig. 6 - Assumed radial load-deflection characteristics of tires (flat terrain)

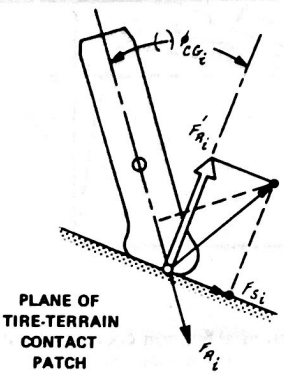

ϕ_{CG_i} = CAMBER ANGLE RELATIVE TO TERRAIN (SHOWN NEGATIVE)

F_{S_i} = SIDE FORCE PRODUCED BY COMBINATION OF SLIP ANGLE AND CAMBER ANGLE

i = 1, 2, 3, 4

Fig. 7 - Vector summation of forces with components along line of action of radial tire force (viewed from rear)

the current time increment, an iterative procedure is employed to correct both F'_{R_i} and F_{S_i}.

Calculation of Circumferential and Side Forces - The analytical treatment of circumferential and side forces that was used in Ref. 1, wherein application was made of the nondimensional slip angle variable and the "friction circle" concept of Ref. 10, has been modified to suit the needs of the present simulation. The planned applications require that the relationship between rotational slip and circumferential forces be simulated and that interactions between circumferential and side forces be treated with greater accuracy than that provided by the "friction circle." The selected analytical representation, which makes use of tabular inputs of the circumferential force characteristics of tires to permit the direct application of measured data, constitutes a varying "friction ellipse" (Fig. 8). The ratio of the major axis (maximum circumferential friction force) to the minor axis (maximum side friction force) is a function of vehicle speed. The magnitude of the minor axis is a function of both vehicle speed and tire loading. Where surface water is present, its effects are reflected in the tabular inputs for the magnitude of the minor axis. The basis for selection of this analytical representation is presented in the following paragraphs.

Pertinent Measured Behavior of Tires - The side force calculations are based on empirical fits to measured small-angle properties of the tires, which become "saturated" at large angles. Variations in the small-angle cornering and camber stiffnesses, that are produced by changes in tire loading, are approximated by parabolic curves fitted to experimental data.

The general form of variation of the effective circumferential friction coefficient as a function of rotational slip is well established (Fig. 9). Although specific applicable data are relatively sparse, significant recent contributions have been made by Krempel (13) and Gengenbach (14). The test results presented in Refs. 13 and 14 are, of course, for particular tires and operating conditions. It is not possible, therefore, to generalize the behavior of tires on the basis of those test data. However, they do indicate the sort of properties that must be accommodated in the present simulation program.

For purposes of the present simulation, the simplifying assumption has been made that the peak value of the friction coefficient for side forces, designated by μ_i, is equal to the circumferential friction coefficient, μ'_i, under the condition of full sliding (that is, 100% rotational slip). With this assumption, plots of experimental data for the circumferential fric-

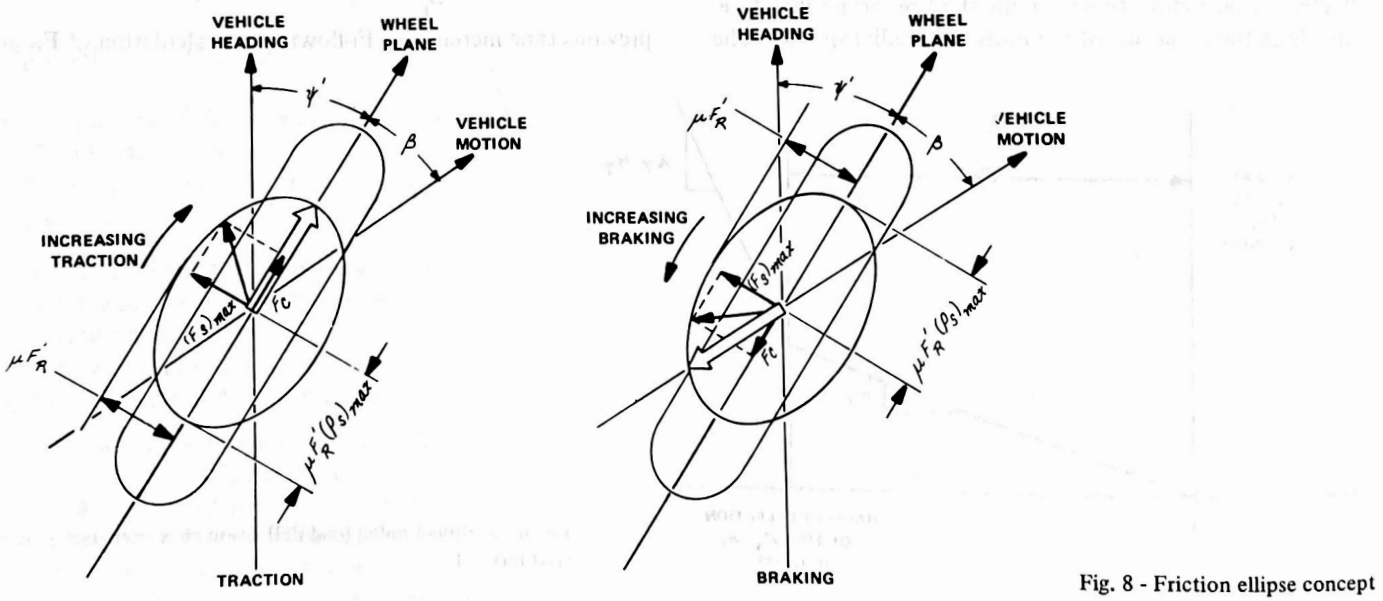

Fig. 8 - Friction ellipse concept

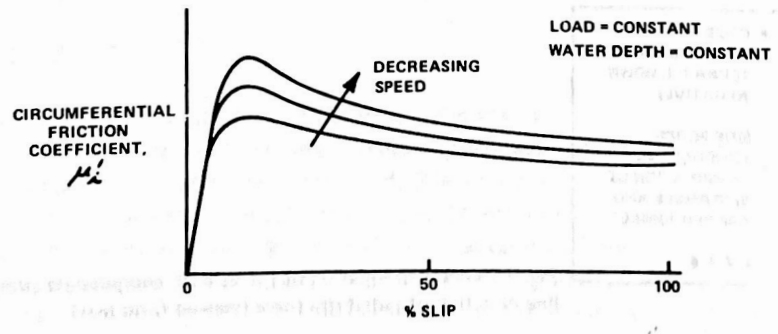

Fig. 9 - Variation of circumferential friction coefficient with rotational slip and speed

tion coefficient versus rotational slip and speed (Fig. 9) can be converted to plots of the ratio ρ_{S_i} (Fig. 10), where:

$$\rho_{S_i} = \frac{\mu_i'}{\mu_i} = \frac{F_{C_i}}{\left(F_{S_i}\right)_{max}} \qquad (2)$$

On the basis of pertinent data presented in Ref. 14, it has been further assumed that the effects of rotational slip, speed, tire loading, and water depth, can be adequately approximated by a combination of appropriate variations of μ_i with speed and tire loading, and of the ratio, ρ_{S_i}, with speed and rotational slip.

For dry pavement, Ref. 13 indicates linear variation of the peak friction coefficients with speed, as depicted in Fig. 11. It has been assumed for purposes of estimating input data that the relationship between $(\mu_i')_{max}$ and μ_i, as depicted in Fig. 11, is also approximately correct for wet pavement.

Input Requirements -

1. 6 X 6 table of $(RATIO)_i = f\left(\sqrt{U_{G_i}^2 + V_{G_i}^2}, F'_{R_i}\right)$

where:

$$(RATIO)_i = \begin{cases} \dfrac{\mu_i}{AMU}, & \text{for wheel i outside of terrain tables} \\ \dfrac{\mu_i}{AMUG(n)}, & \text{for wheel i inside of terrain table n} \end{cases}$$

AMU, AMUG(n) = Tire-terrain friction coefficients corresponding to zero speed and nominal tire loading

$\sqrt{U_{G_i}^2 + V_{G_i}^2}$ = Resultant speed of the contact point of wheel i in the tire-terrain contact plane

These inputs correspond to a given pavement condition (that is, dry, or some specific depth of water). For each wheel, the tabular inputs are interpolated for the instantaneous values of resultant speed in the tire-terrain contact plane, $\sqrt{U_{G_i}^2 + V_{G_i}^2}$, and tire load, F'_{R_i}, to obtain $(RATIO)_i$. The value of μ_i, the minor axis of the "friction ellipse," is obtained from the preceding definitions of $(RATIO)_i$.

2. 30 X 3 table of $\rho_{S_i} = f[(SLIP)_i, U_{G_i}]$

The instantaneous values of rotational slip, $(SLIP)_i$, and speed, U_{G_i}, are interpolated to obtain the ratio ρ_{S_i}. The major axis of the friction ellipse is determined from

$$\mu_i' = \rho_{S_i}\,\mu_i \qquad (4)$$

Since the pair of drive wheels are coupled in rotational motion through the differential gears, it is necessary to combine the tire force calculations for the front and rear pairs of wheels.

Application of the "Friction Ellipse" Concept (Fig. 8) - The "friction ellipse" is an extension of the "friction circle" concept to provide a more realistic treatment of interactions between the circumferential force (that is, tractive or braking) and the side force of a tire. Experimental evidence that the maximum values of tire friction forces are dependent on direction relative to the wheel plane is presented by Krempel (13). The "friction circle concept is, of course, based on the assumption that such a directional dependence does not exist. The objective of the present development has been to achieve a simple analytical representation that is more accurate than the "friction circle." The selected input format permits direct application of experimental data, where available. Also, by appropriate selection of inputs, the "friction ellipse" can be reduced to a "friction circle" for comparisons of response predictions.

In the "friction ellipse" form of treatment of interactions, the maximum value of the resultant tire friction force in the tire-terrain contact plane is assumed to be bounded by an ellipse with the minor axis equal to $2\mu F'_R$, and major axis equal to $2\mu F'_R\,(\rho_S)_{max}$,

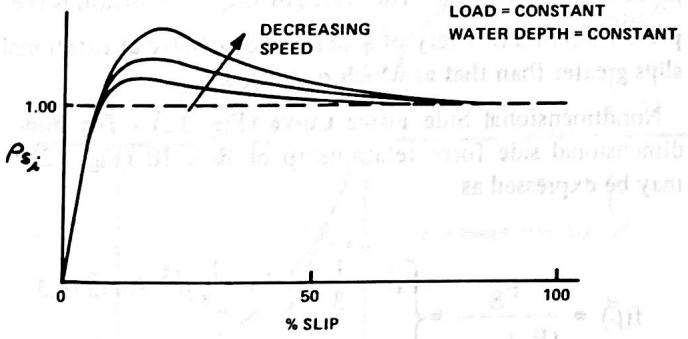

Fig. 10 - Ratio of circumferential friction coefficient to peak side-force coefficient as a function of rotational slip and speed

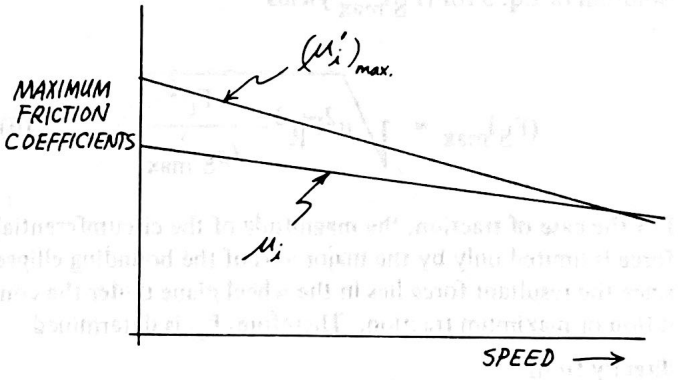

Fig. 11 - Variation of $(\mu_i')_{max}$ and μ_i with vehicle speed

where:

μ = Effective tire-terrain friction coefficient for side forces, for the given conditions of vehicle speed, and tire loading. Note that, in the absence of circumferential forces, the value $\mu F'_R$ constitutes the maximum achievable side force

ρ_S = Ratio of $\frac{\mu'}{\mu}$, for the given conditions of rotational slip and vehicle speed, where μ' is the effective friction coefficient for circumferential forces. Since ρ_S is a function of both rotational slip and vehicle speed, $(\rho_S)_{max}$ corresponds to the rotational slip condition that produces the maximum value of μ' at the given vehicle speed

F'_R = Tire loading perpendicular to the tire-terrain contact plane, lb

The bounding ellipse is depicted in Fig. 8. Note that a value of $(\rho_S)_{max} = 1.000$ will reduce the "friction ellipse" to a "friction circle."

In the calculation procedure of the developed analytical treatment of interactions, the circumferential tire force, F_C, is given first priority in utilization of the available friction. The maximum value of side force, $(F_S)_{max}$, corresponding to a resultant force that constitutes a radius vector of the bounding ellipse, is then determined for use in the calculation of side forces (Fig. 8). Note that this sequence of calculations is identical with those of Refs. 1 and 10 for the "friction circle" concept.

In Fig. 8, the maximum value of side force $(F_S)_{max}$, for a given circumferential force, F_C, is determined in the following manner. The equation of the bounding ellipse may be expressed as

$$(F_S)^2_{max} + \frac{F_C^2}{(\rho_S)^2_{max}} = \mu^2 F'^2_R \tag{5}$$

Solution of Eq. 5 for $(F_S)_{max}$ yields

$$(F_S)_{max} = \sqrt{\mu^2 F'^2_R - \frac{F_C^2}{(\rho_S)^2_{max}}} \tag{6}$$

For the case of traction, the magnitude of the circumferential force is limited only by the major axis of the bounding ellipse, since the resultant force lies in the wheel plane under the condition of maximum traction. Therefore, F_C is determined directly from

$$F_C = \rho_S \mu F'_R \tag{7}$$

In the case of braking, where the limiting condition on the resultant force is that of opposing the direction of vehicle motion, the maximum circumferential force may be less than $\rho_S \mu F'_R$. Therefore, the circumferential component corresponding to the cited limiting condition on the resultant force is calculated, as follows, for comparison with $\rho_S \mu F'_R$, and the smaller of the two values (that is, smaller absolute value) is used in Eq. 6. From Eq. 5, and inspection of Fig. 8,

$$F_C^2 + (F_S)^2_{max} = \mu^2 F'^2_R + F_C^2 \left[1 - \frac{1}{(\rho_S)^2_{max}}\right] = F_C^2 \sec^2\beta \tag{8}$$

Solution of Eq. 8 for F_C yields

$$F_C = \frac{\mu F'_R}{\sqrt{\tan^2\beta + \frac{1}{(\rho_S)^2_{max}}}} \tag{9}$$

Thus, the calculation of F_C, to treat either traction or braking, is as follows:

$$F_C = \begin{cases} \rho_S \mu F'_R \\ \text{or} \\ \dfrac{\mu F'_R}{\sqrt{\tan^2\beta + \dfrac{1}{(\rho_S)^2_{max}}}} \end{cases} \tag{10}$$

whichever has the smaller value. Application of the value of F_C obtained from Eq. 10 in Eq. 6 yields the required value of $(F_S)_{max}$.

The preceding calculation procedure is applied for all values of rotational slip less than that which produces the value $(\rho_S)_{max}$. For rotational slips greater than that corresponding to $(\rho_S)_{max}$, Eqs. 6 and 10 are modified by the substitution of ρ_S to replace $(\rho_S)_{max}$. The effect of this substitution is the prevention of a recovery of side force capability at rotational slips greater than that at which $\rho_S = (\rho_S)_{max}$.

Nondimensional Side Force Curve (Fig. 12) - The nondimensional side force relationship of Ref. 10 (Fig. 12) may be expressed as

$$f(\bar{\beta}) = \frac{F_S}{(F_S)_{max}} = \begin{cases} \bar{\beta} - \frac{1}{3}\bar{\beta}|\bar{\beta}| + \frac{1}{27}\bar{\beta}^3, \text{ for } |\bar{\beta}| < 3 \\ 1, \text{ for } 3 \leq |\bar{\beta}| \end{cases} \tag{11}$$

where:

F_S = Actual side force

$(F_S)_{max}$ = Maximum achievable value of side force, as limited by Eq. 6

$$\bar{\beta} = \frac{F'_S}{(F_S)_{max}}$$

F'_S = Side force value corresponding to small-angle properties of the tire

To permit the use of the nondimensional slip angle variable which "saturates" the side force at large slip angles, an "equivalent" slip angle is used to approximate camber effects.

Wheel Aligning Torques - Aligning torques on the front wheels are simulated by means of a constant "pneumatic trail" dimension when the steer-mode degree of freedom is activated.

TERRAIN PROFILE

Provisions for entry of terrain profile data, for simulation of the traversal of uneven terrain, have been revised to permit the detailed definition of long and narrow strips of roadway. Outside the ranges of the tabular inputs of data, the terrain is treated as a flat, horizontal plane. Note that the tabular input format is used only for the case of point-contact representation of the tires.

The developed treatment of the terrain profile permits use of as many as five separate tables for specification of terrain elevations. Four of the tables are constant-increment tables for X′ and Y′. The fifth is a variable-increment table which requires specification of the X′ and Y′ values of the grid, in addition to the terrain elevations, as input data. Unlike the former method, tabular values of terrain slopes are not entered as inputs. Rather, these quantities are now automatically computed in the program from the terrain elevation data.

The program provides for overlapping of the tables. Thus, for example, a "fine mesh" table may be used to provide greater detail of a section of terrain that is located within the bounds of one or more "coarse mesh" tables. In addition, different friction coefficients for the ground surface defined in each table may be specified.

In Fig. 13, the analytical representation of curb profiles is depicted. Three planes are defined, with lines of intersection parallel to the space fixed X′ axis. A separate friction coefficient, μ_c, is defined for the curb facing. The wheels that are not in contact with the curb are treated as being on a flat,

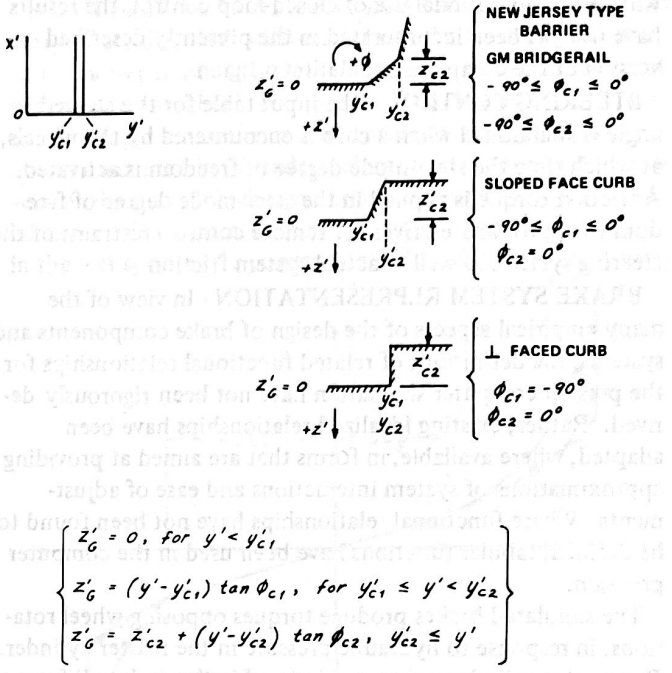

$$\begin{cases} z'_G = 0, & \text{for } y' < y'_{c1} \\ z'_G = (y' - y'_{c1}) \tan \phi_{c1}, & \text{for } y'_{c1} \le y' < y'_{c2} \\ z'_G = z'_{c2} + (y' - y'_{c2}) \tan \phi_{c2}, & y'_{c2} \le y' \end{cases}$$

Fig. 13 - Analytical representation of curb profiles

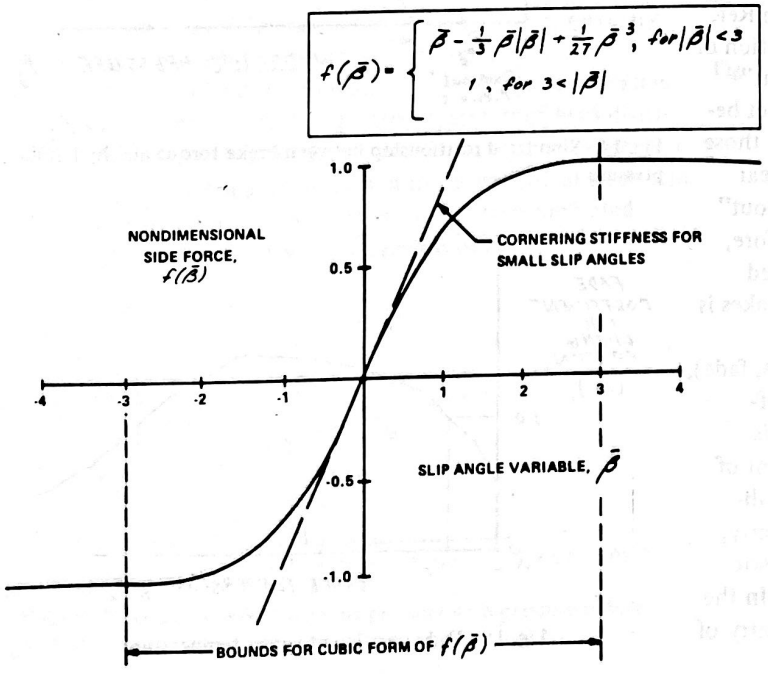

Fig. 12 - Nondimensional tire side-force curve

horizontal plane, with the specified ground friction coefficient, AMU.

CONTROL INPUTS

Open-loop control inputs in the form of the steer angle at the front wheels (assumed to be equal at the two wheels), the throttle setting, the hydraulic pressure in the brake system master cylinder, and the transmission ratio, are entered as arbitrary tabular functions of time, which are interpolated in the calculation procedure. While some preliminary work has been performed on the development of a subroutine for modeling the responses of a driver to sensory inputs (9), which will permit an optional use of closed-loop control, the results have not yet been incorporated in the presently described version of the computer simulation program.

STEERING CONTROL - The input table for the steered angle is abandoned when a curb is encountered by the wheels, at which time the steer-mode degree of freedom is activated. A friction torque is applied in the steer-mode degree of freedom to approximate driver (or remote control) restraint of the steering system, as well as actual system friction.

BRAKE SYSTEM REPRESENTATION - In view of the many empirical aspects of the design of brake components and systems, the definitions of related functional relationships for the present computer simulation have not been rigorously derived. Rather, existing idealized relationships have been adapted, where available, in forms that are aimed at providing approximations of system interactions and ease of adjustments. Where functional relationships have not been found to be defined, tabular functions have been used in the computer program.

The simulated brakes produce torques opposing wheel rotations, in response to hydraulic pressure in the master cylinder. The master cylinder pressure is entered in "open-loop" form as an input tabular function of time.

The analytical relationships for brake torque versus hydraulic pressure are based on corresponding expressions given in Ref. 15. Modifications of the relationships, to permit simulation of fade effects and of the torque lag produced by "push-out" pressure (that is, the pressure required to produce contact between the shoe and the drum or disc), are identical with those of Ref. 16. In each expression, the brake torque is a linear function of the excess of actuation pressure over "push-out" pressure, at a given brake temperature (Fig. 14). Therefore, the only justification for the use of relatively complicated analytical relationships for the four optional types of brakes is their capability of approximating fade effects.

The effects of elevated temperatures on brakes (that is, fade), particularly on brakes that include a large amount of self-actuation, are not known to be defined analytically. It is known, of course, that the "effective" friction coefficient of the lining material changes with temperature, but an established predictive technique is not known to exist. Similarly, the rate of heat dissipation by the brake assembly does not appear to be defined by a general analytical treatment. In the manner of Ref. 16, provisions have been made for the entry of coefficients of heat transfer, specific heats, effective masses of heated parts, and for the tabular entry of a fade coefficient for the brake lining as a function of brake temperature (Fig. 15). If such data either are available or can be estimated, the simulation provides an approximate treatment of dynamic fade effects based on time-history calculations of the energy dissipation at the individual brakes. Note that the availability of experimental data on the time history of brake temperatures during brake tests will permit an empirical adjustment of these inputs, to produce a "realistic" variation of calculated temperatures in the simulation. The fade effects can be suppressed, if desired, by selection of appropriate input data.

While nearly all United States automobiles have a fixed distribution of braking effort, a variety of control devices have been and are being developed for varying the distribution of braking effort. The present simulation includes provisions for simulation of pressure-reducing devices.

Brake pressure-reducing devices (for example, Kelsey-Hayes proportioning valve (16)) produce a ratio of rear/front hydraulic pressure of less than 1.00 when a preselected master cylinder pressure is exceeded. Some valves of this type include more than one such step change in rear/front pressure ratio. In Fig. 16, a plot of rear versus front hydraulic pressure is presented for this type of device.

The wide variety of proposed and existing control systems for antiskid brakes will make necessary the development of

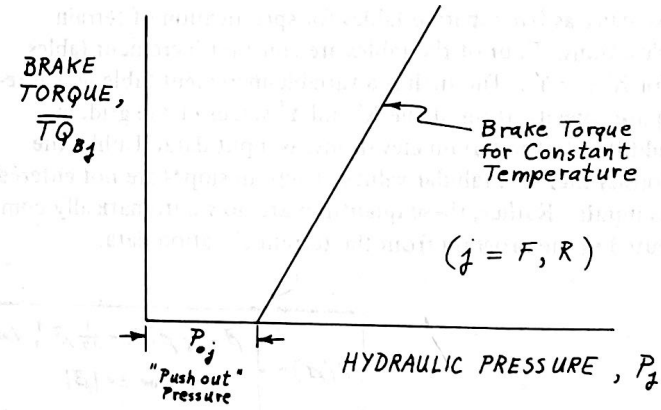

Fig. 14 - Simulated relationship between brake torque and hydraulic pressure

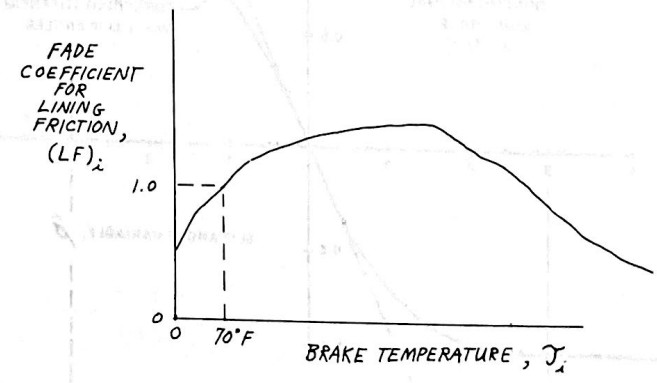

Fig. 15 - Fade coefficient versus temperature

special subroutines for each type of system. The comprehensive definition of response details that are provided by the modified simulation program, along with the capability of exact repetition of operating conditions, constitutes a unique capability for comparative evaluations and for studies of control system optimization.

TRACTIVE EFFORT ASPECTS - The primary objectives of the analytical selections related to the vehicle driveline have been to approximate the effects of engine braking and to limit the applied tractive torques to values compatible with the vehicle speed and engine power. Note that the previous form of open-loop operation (1) could result in the application of excessive torques, through the lack of precise knowledge of the vehicle speed that will exist at a given point in time.

The violent maneuvers and accident-related events that can be studied with the present computer simulation are generally of short duration and the need for a capability of shifting gears during a run is considered to be of secondary importance. However, in view of the relative ease of including a declutching and gear changing option, these items have also been incorporated.

The engine torque is interpolated, for engine speed and for throttle setting, from corresponding tabular inputs. The instantaneous engine speed is determined from the transmission ratio and the speed of the propeller shaft corresponding to the instantaneous values of rotational speeds of the driving wheels. For engine speeds thus determined, that are less than or equal to 500 rpm, the transmission ratio is set to zero, simulating a disengagement of the clutch. The throttle setting is entered as a tabular function of time. It is assumed that the engine torque increases linearly with throttle setting between the values entered for closed throttle and for wide open throttle.

SUSPENSION PROPERTIES

The simulated load-deflection properties of the suspensions, effective at the wheels, include: linear elastic rates; nonlinear, energy-dissipating, deflection-limiting stops; elastic auxiliary roll stiffness; coulomb friction; and viscous damping.

DEFLECTION-LIMITING STOPS - For the present version of the simulation, in which the detailed effects of load distribution and suspension "strike through" are of interest, several refinements have been incorporated in the analytical treatment of the suspension bumpers. The refinements in simulated bumper properties are based on a review of available experimental data (for example, Ref. 17). They include progressively stiffening load-deflection rates and an adjustable amount of energy dissipation (note that data presented in Ref. 17 indicate that as much as 50% of the energy absorbed by a "typical" bumper may be dissipated). Provision has also been incorporated for unsymmetrical placement of the jounce and rebound bumpers with respect to the design positions of the wheels.

In order to accurately define the characteristics of suspension stops, the directly related inputs have been extended to include seven items per end of the vehicle. The combined spring and bumper forces are calculated in the manner depicted in Fig. 17.

AUXILIARY ROLL STIFFNESS - Provision is made for the entry of auxiliary roll stiffness at both the front and the rear suspensions (that is, roll stiffness in excess of that corresponding to the front wheel rates in ride and to the rear spring rates and spacing). While the antiroll torsion bar, which is frequently included in the independent front suspensions of conventional automobile designs, constitutes an obvious form of auxiliary roll stiffness, it should be noted that torsional effects in the leaf springs of a conventional Hotchkiss rear suspension

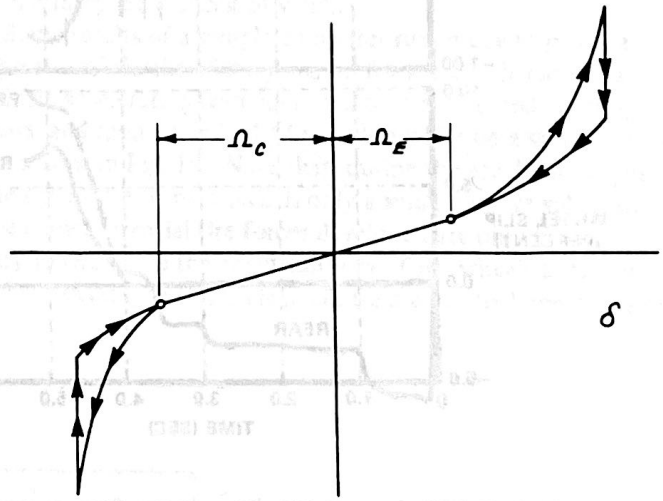

Fig. 17 - General form of simulated suspension bumper characteristics

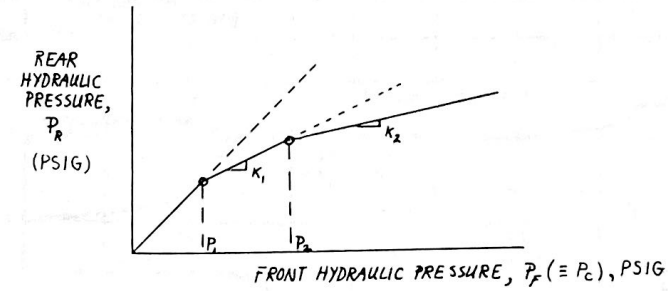

Fig. 16 - Rear versus front hydraulic pressure with pressure-reducing device

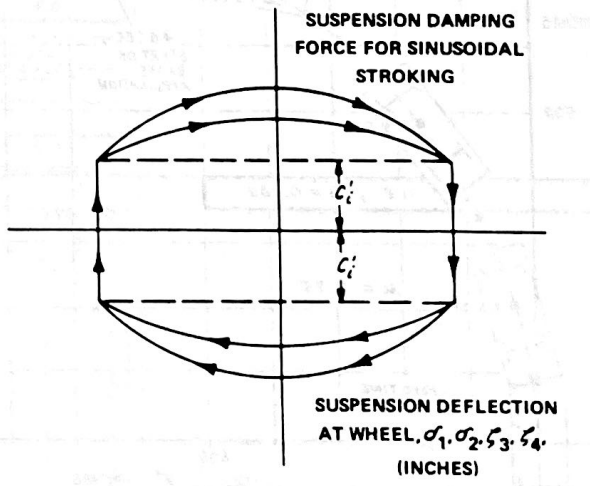

Fig. 18 - Assumed form of suspension damping

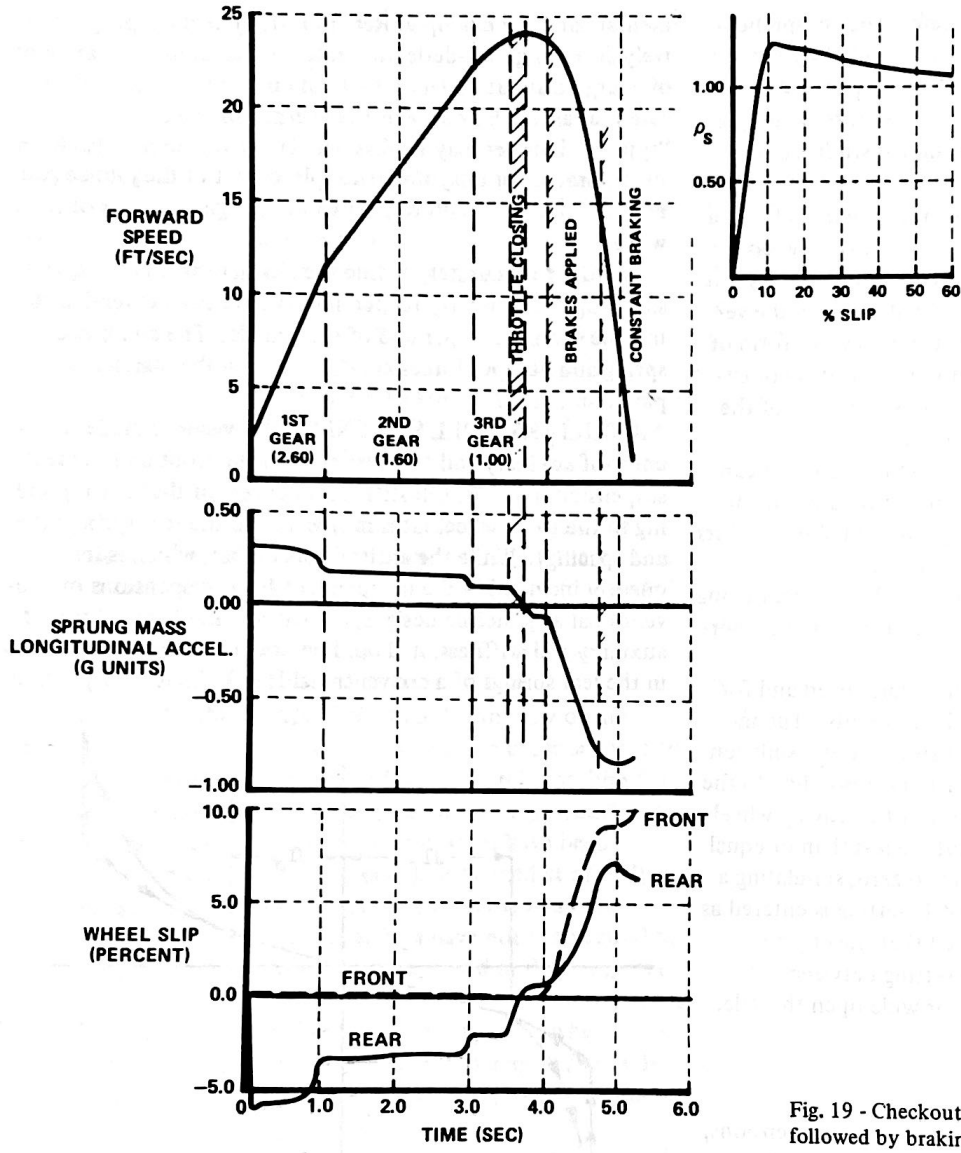

Fig. 19 - Checkout run results: Acceleration from low speed followed by braking

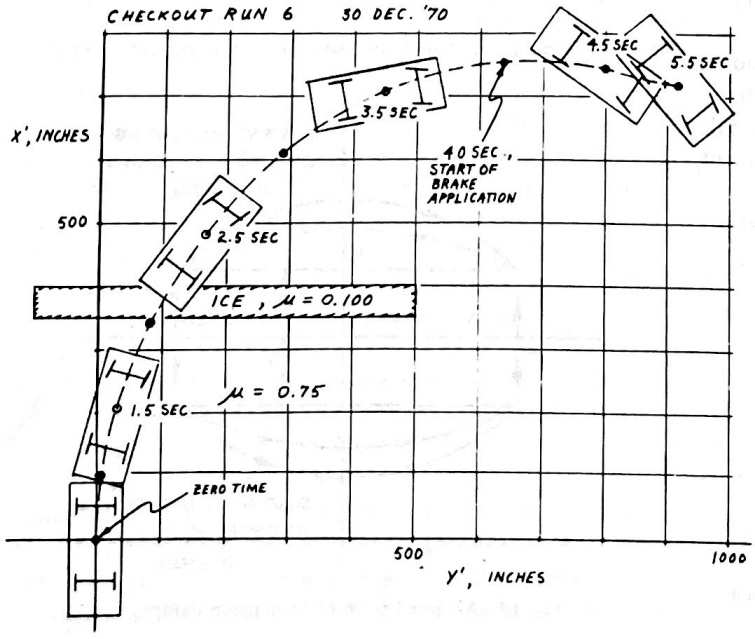

Fig. 20 - Vehicle trajectory

also produce a significant amount of auxiliary roll stiffness, as here defined.

SUSPENSION DAMPING - The assumed form of damping is depicted in Fig. 18. The coulomb friction, C_i', is used to approximate the combination of "blow-off" type damping in the shock absorbers and actual friction in the suspension.

ROLLING RESISTANCE AND AERODYNAMIC DRAG

The combined effects of rolling resistance and aerodynamic drag are grossly approximated by means of a force applied directly to the sprung mass. An empirical relationship is used to approximate the magnitude of the applied force as a function of the first and second powers of the longitudinal component of vehicle velocity. It is assumed, for simplicity, that the motion-resisting force acts through the c.g. of the sprung mass, and along the longitudinal axis of the vehicle (the X axis), in the direction opposite to that of the longitudinal component of vehicle velocity. The primary objective of this simplified analytical treatment is to approximate the effects of aerodynamic and rolling resistances on stopping distances.

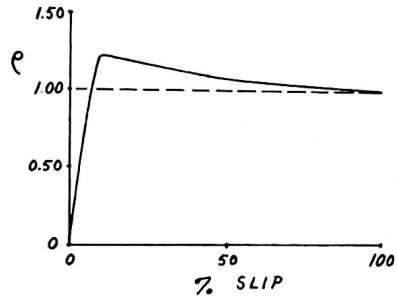

Fig. 21 - Assumed tire friction ratio versus rotational slip

DISCUSSION OF RESULTS

At the time of preparation of this paper, all of the detailed options—the different types of brakes, brake fade, variation of friction coefficient with speed, etc.—have not yet been tested. However, on the basis of sample runs performed for checking purposes, it is considered that development of the basic program has been completed.

Initial checking consisted of comparisons of predictions for straight-ahead braking with those of an earlier, planar simulation (16). The planar simulation has not been rigorously validated, but it has been shown to agree closely with available, albeit fragmentary, experimental data. Also, its output includes a comprehensive summary of the instantaneous distribution of system energy, which has provided verification of the absence of errors, and of its consistency with the physical laws (that is, the total system energy remains constant, while it is being redistributed during a braked stop). With matched inputs, the extended vehicle simulation has been shown to yield results that are identical with those of the planar simulation, in straight-ahead stops. This fact does not establish detailed validity, of course, but it does serve as an excellent, preliminary gross check of validity.

Some results of a sample computer run, made to provide operational checks of the program for the simple case of a vehicle accelerating from an initial near-zero speed, shifting gears, and then being braked to a stop while on a straight path, are shown in Fig. 19. Note that, during the acceleration phase, the slip of the front wheels is only a small positive value, since the circumferential tire forces developed are only those necessary to overcome the angular inertia of the wheels as the vehicle increases speed. This is in contrast with the large negative

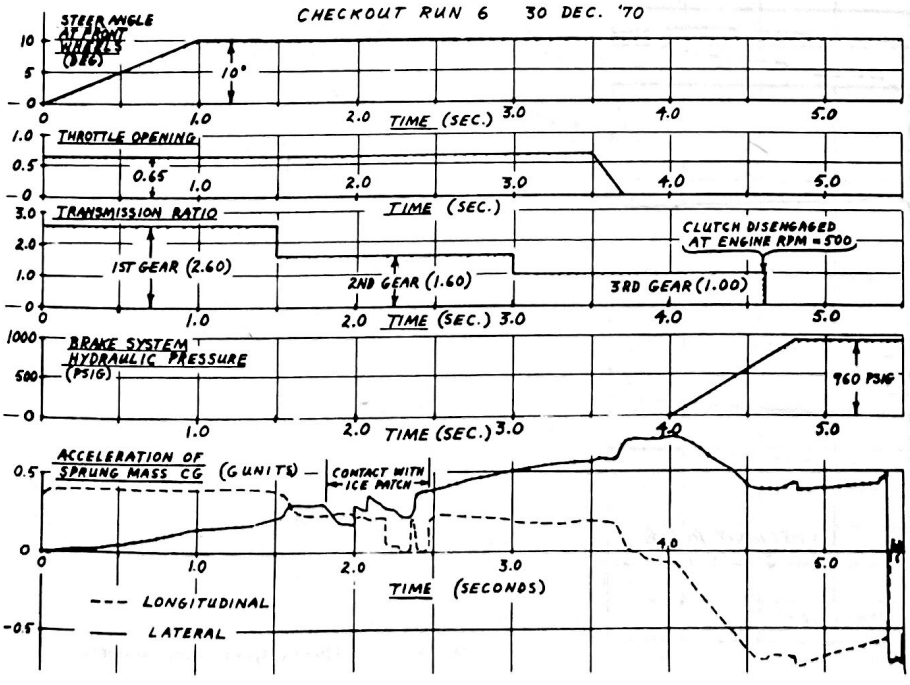

Fig. 22 - Control inputs and sprung mass acceleration

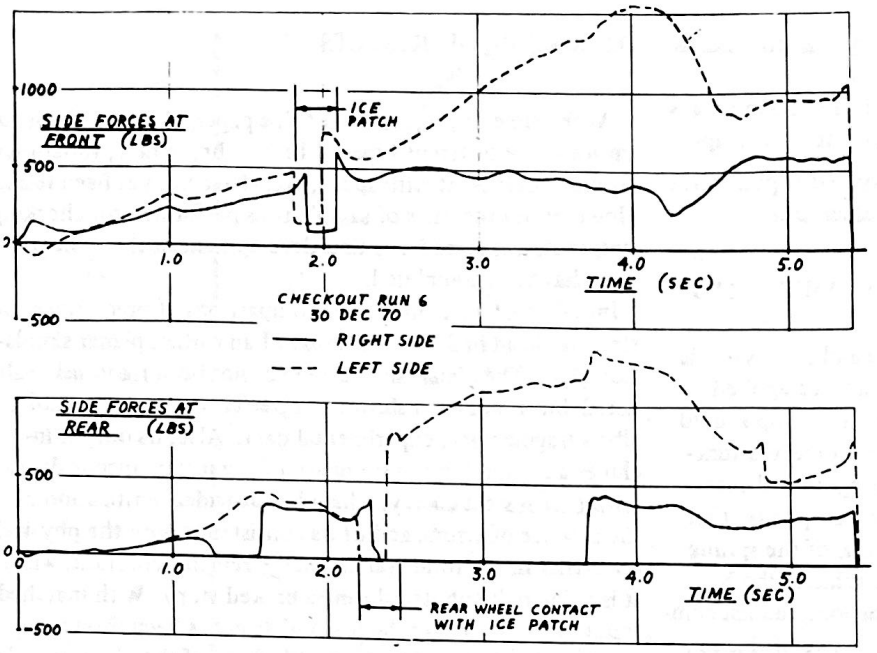

Fig. 23 - Tire side forces

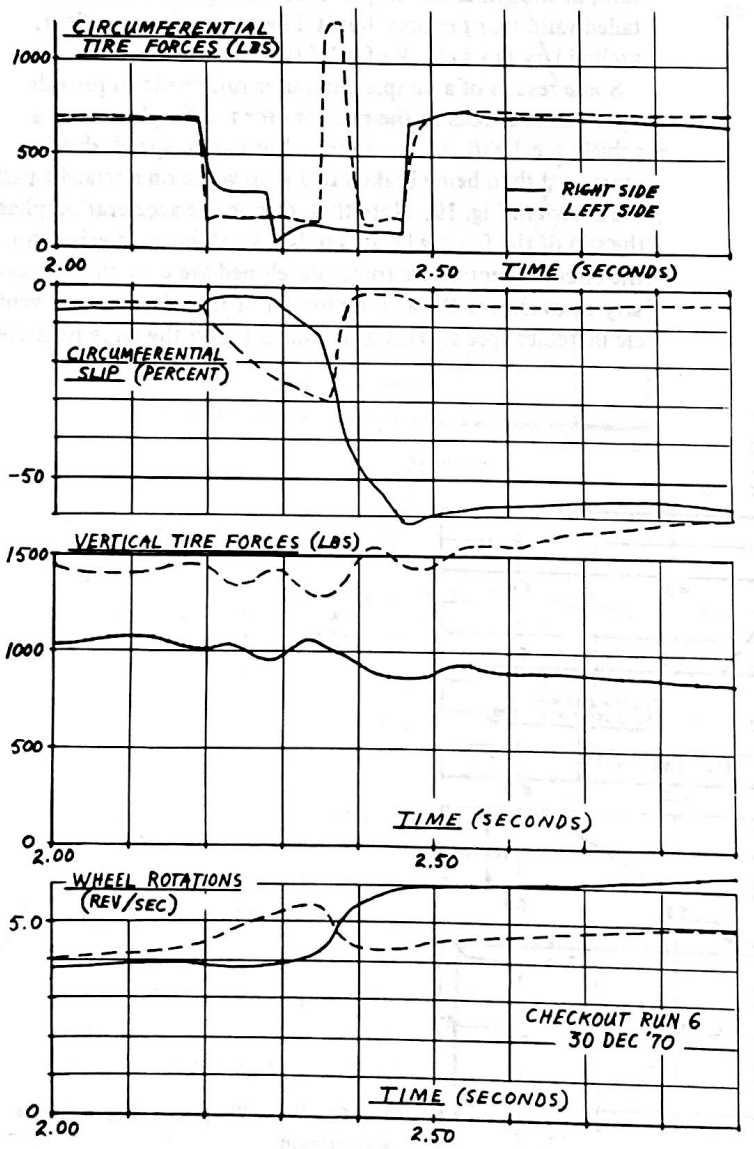

Fig. 24 - Rear wheel responses on ice patch

slips of the rear wheels which develop traction forces to accelerate the vehicle. The slips of both the front and the rear wheels change rapidly to relatively large positive values when the brakes are applied. It may also be noted that the effects of engine braking are evidenced in the simulation results during the short period of closed throttle between 3.7 and 4.0 sec.

For traction or braking, combined with cornering, a current lack of applicable experimental data has limited the checking process to numerical checks of the predicted tire forces, to establish that the derived analytical relationships are being correctly implemented, and to qualitative evaluations of the predicted vehicle behavior. In Figs. 20-25, time histories of predicted responses in one such check run are displayed. The depicted run consists of an acceleration, including gear changes, while cornering on a flat surface that contains a patch of ice.

Fig. 20 depicts the predicted vehicle trajectory. The assumed relationship between the friction ratio–circumferential divided by side–and circumferential slip is shown in Fig. 21. Note that the variation of this ratio with vehicle speed has, for simplicity, not been included in the inputs of the displayed check run. In Fig. 22, the control inputs and the predicted acceleration components of the sprung mass are displayed. Fig. 23 depicts the time histories of the tire side forces, while Figs. 24 and 25 display the detailed responses of the individual wheels during traversal of the ice patch, followed by a brake application.

In Fig. 25, the front wheel responses are displayed on enlarged scales, since the circumferential slips and forces are relatively small, corresponding only to rotational accelerations of the individual wheels. The circumferential slips are seen to rapidly increase on the ice until the force levels required to maintain the rates of wheel accelerations are achieved. The seemingly erratic behavior of the small circumferential forces, subsequent to contact with the ice, reflects the effects of changes in both the tire loads and the rolling radii, as well as dynamic overshoot of equilibrium values.

On the basis of the check runs made to date, it is concluded that the basic program (exclusive of the untested options) is correctly implementing the developed analytical relationships and that gross indications of validity have been achieved. The next phase of checking will be combined with a program of

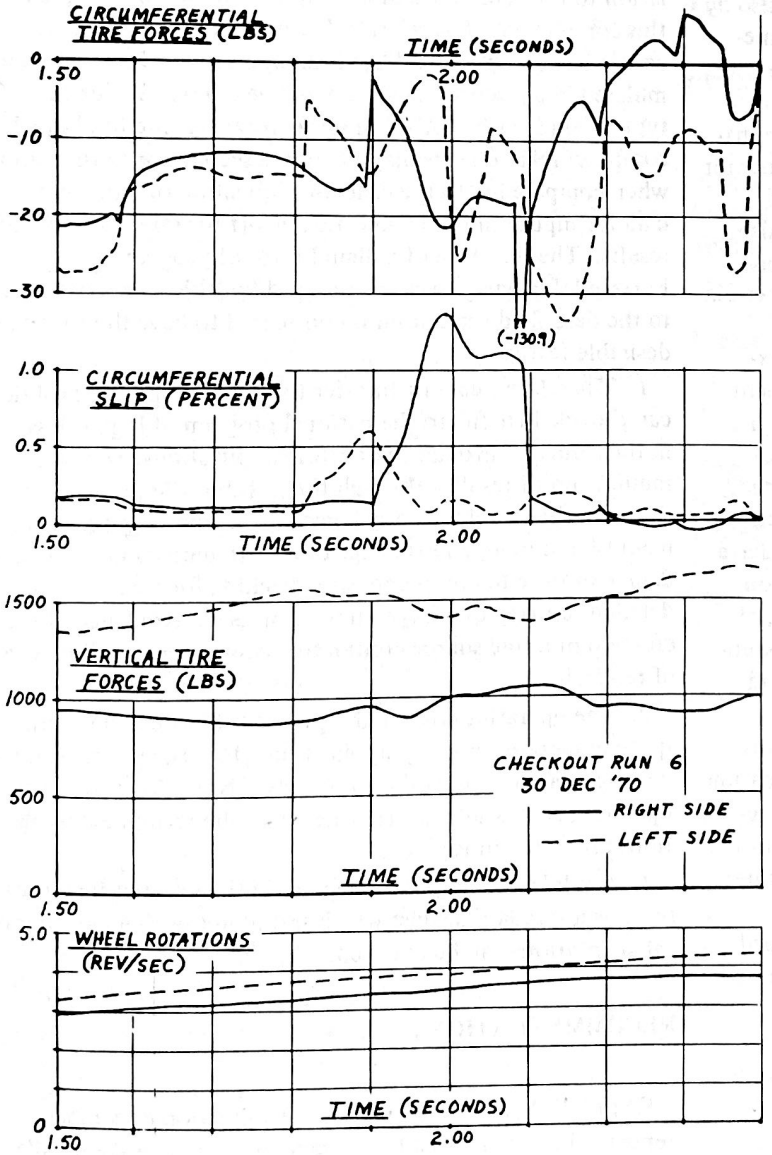

Fig. 25 - Front wheel responses on ice patch

rigorous validation in which direct comparisons can be made with experimental data.

CONCLUSIONS

CAPABILITIES - The computer simulation that has been developed within this research task is uniquely suited for studies of the performance of braking systems, and of the driving task, under realistic operating conditions.

The capability of the developed simulation for treating the detailed dynamics of combined cornering and braking on pavement with surface irregularities and/or nonuniform friction properties, as well as the linear ranges of operation, permits the extension of analytical studies to realistic operating conditions similar to those under which control loss occurs in actual highway accidents. While simplified, linearized analyses may be somewhat more elegant and more satisfying to the analyst, it must be recognized that the actual real-world dynamic system includes complex and subtle interactions (for example, the changing distribution of tire loading during combined braking, cornering and ride motions which are affected also by the nonlinear characteristics of antipitch suspension geometries, the effects of the differential gears and of driveline inertia on the occurrence of rear wheel lock-up, etc.). Arbitrary omissions of such system details prior to the determination of the importance of their interactions, in order to permit the performance of "simple and direct" analyses, can, of course, lead to unrealistic and misleading conclusions. Also, it should be noted that nonlinear effects are frequently encountered under "normal" operating conditions such as terrain discontinuities produced by pavement settling.

VALIDITY - Response predictions obtained with the extended simulation have been shown to be in gross agreement with experimental data, and it is fully expected that a high degree of detailed correlation with experiments will be achieved when a rigorous validation study can be performed.

While the extended simulation program has not yet been rigorously validated, the detailed predictions of behavior have been found to be qualitatively correct. Also, the validation study performed with the basic BPR-CAL simulation (1), of which the presently reported simulation constitutes an extension and refinement, provides evidence of remarkably good correlation of predicted and experimentally measured responses, despite the fact that the earlier treatments of many aspects of the system (for example, braking system, suspension bumpers, etc.) were quite crude by comparison. It is, therefore, fully expected that a high degree of detailed correlation with experiments will be achieved in future validation studies with the present simulation program.

OPERATING COST - The operating cost of the developed digital computer program is considered to be quite moderate for many anticipated applications.

The operating cost of the extended digital simulation program has been found, in the limited number of runs performed to date, to constitute an increase over that of the basic BPR-CAL program (1) by a factor between 1.50-3.13. The indicated range of the factor, which corresponds to operating costs between \$6.00-12.50/sec of simulated time, using the CAL computer facility, was found to apply when time intervals ranging from 0.005-0.010 sec were used in check-out runs. Since the smaller selections of time interval size were based on the desired intervals of output for checking purposes, rather than on requirements for solution stability, they are probably smaller than the time interval needs of any application runs. Therefore, the operating cost in applications will undoubtedly be less than \$12.00/sec.

The extensions and refinements that are described herein have been programmed with straightforward Fortran IV coding, for ease of transfer to other computing facilities, with only secondary consideration given to operating time and costs. If primary attention were to be given to economics, as opposed to ease of transfer, it is believed that the cost factor in relation to the basic program could be reduced to the range of 0.75-1.50 in a purely digital program (that is, an operating cost between \$3.00-6.00/sec of simulated time) or to a substantially lower value in a hybrid adaptation.

There are a number of factors that must be considered in relation to the economics of a computer simulation program of this complexity. The relationship between the setup costs of a computer simulation and the total operating costs to be accumulated in a given application must be considered for each type of application. Also, in some instances, the total of all computer-related costs may be only a secondary consideration when compared with the costs of acquisition of parameter data for inputs and of engineering effort for interpretation of results. The selection of a digital form of program, in the Fortran IV language, was encouraged by BPR. This approach to the described simulation is considered to have the following desirable features:

1. The relative ease of transfer to other computing facilities can provide benefits to the national program of highway safety in the form of: avoidance of effort duplications; ease of communication of results—through the possible widespread adoption of uniform reference systems and terminology; encouragement of a more open exchange of experimental and analytical data; exposure to comprehensive checking for errors via the detailed scrutiny of a large number of users; avoidance of the creation of a sole source contractor requirement for this type of research.

2. The operating cost of the program in its existing form, is quite moderate for many applications (that is, applications involving relatively short duration runs). Note that the actual operating cost is substantially less than the related extrapolations presented in Ref. 18.

3. A validated computer program in the selected format can serve as a standard against which faster and/or more economical adaptations can be checked.

RECOMMENDATIONS

EXPERIMENTS - The program of validation experiments reported in Ref. 1 should be extended to include the detailed

response measurements necessary for validation of the presently reported simulation modifications.

Additional instrumentation should be installed in the test vehicle to measure rotational velocities of the individual wheels, driveline torque, brake system hydraulic pressure, etc., in order that the validity of the detailed extensions of the simulation can be investigated. In addition to detailed comparisons of predicted and measured responses for a standard vehicle, it would be highly desirable to also modify the test vehicle to include commercially available braking system devices such as the Kelsey-Hayes proportioning valve and the Ford antiskid system, to permit further response comparisons for validation purposes. Note that response predictions with the Ford antiskid system will require the development of a relatively simple special subroutine to simulate the modulation of actuation pressure at the rear brakes.

DESIGN CALCULATIONS - Following validation, the developed computer simulation should be applied to explore the extent of inaccuracies in current simplified design calculations that may stem from the effects of terrain irregularities, vehicle cornering, nonuniform pavement friction, brake fade effects, antipitch suspension geometries, etc.

Existing design calculations for braking systems (for example, those presented in Ref. 19) involve extensive simplifications of vehicle dynamics. An exploration of the degree to which the results of such simplified calculations might be inappropriate to realistic operating conditions would appear to be of particular value in relation to the development of performance improvements and to the establishment of requirements for motor vehicle safety standards.

ANTISKID SYSTEMS - The validated simulation program should be applied in evaluations of existing and proposed antiskid braking systems.

The development of relatively simple, special subroutines for modulating brake application pressures, in accordance with the performance of specific skid-control systems, will make the simulation uniquely suited for analytical studies of antiskid braking systems under realistic operating conditions.

DRIVER MODEL - The previously reported "preview-predictor" driver model (9) should be adapted to the extended simulation for further development and for investigation of its validity.

The development of the cited driver model has been aimed at providing a capability to generate representative and realistic driver-control inputs, in simulated emergency and precollision situations, for use in studies related to improvement of the performance of roadside elements in single vehicle accidents. Therefore, a general and readily adjustable driver model, including decision-making capabilities and thresholds of perception, was developed to process and act on relatively comprehensive sensory inputs. The fully developed driver model will permit study of the driving task at the upper limits of control, as well as under normal conditions of operation.

This recommended application, in which a substantial amount of computer operation time–simulated time–is expected to be required subsequent to the development phase, is one which would benefit from a hybrid adaptation of the overall simulation program. The initial, developmental digital version can provide sample runs for checking such an adaptation.

GENERALITY - To increase the generality of the simulation program, provisions should be incorporated for an optional independent rear suspension, for different tire pressures at the individual wheels, and for an automatic transmission (that is, to permit simulation of the corresponding engine braking effects).

ACKNOWLEDGMENTS

The author wishes to acknowledge contributions of the following individuals to the research program described in this paper. For engineering aspects of the computer simulation, thanks to Norman J. DeLeys, Transportation Research Dept., Cornell Aeronautical Lab., Inc.; for computer programming, thanks to Mrs. Camille F. Bainbridge and Charles T. Ryan, Jr., Computer Mathematics Dept, Cornell Aeronautical Lab., Inc.; for planning and reporting, thanks to Dr. John Eicher, Traffic Systems Div., Bureau of Public Roads.

REFERENCES

1. R. R. McHenry and N. J. DeLeys, "Vehicle Dynamics in Single Vehicle Accidents–Validation and Extensions of a Computer Simulation." CAL Report VJ-2251-V-3, December 1968.

2. R. R. McHenry, "An Analysis of the Dynamics of Automobiles During Simultaneous Cornering and Ride Motions." Proceedings of the Symposium on Handling of Vehicles Under Emergency Conditions, Inst. of Mech. Engrs., Loughborough: University of Technology, Jan. 8, 1969.

3. N. J. DeLeys, "Validation of a Computer Simulation of Single Vehicle Accidents by Full-Scale Testing." First International Conference on Vehicle Mechanics, Detroit: Wayne State University, July 1968.

4. R. R. McHenry, D. J. Segal, and N. J. DeLeys, "Determination of Physical Criteria for Roadside Energy Conversion Systems." CAL Report VJ-2251-V-1, July 1967.

5. R. R. McHenry, D. J. Segal, and N. J. DeLeys, "Computer Simulation of Single Vehicle Accidents," Proceedings of the 11th Stapp Car Crash Conference, New York: Society of Automotive Engineers Inc., 1967.

6. C. M. Theiss, "Perspective Picture Output for Automobile Dynamics Simulation." CAL Report VJ-2251-V-2R, January 1969.

7. C. M. Theiss, "Computer Graphics Displays of Simulated Automobile Dynamics." Boston: Spring Joint Computer Conference, May 1969.

8. E. E. Larrabee, "Automobile Dynamics–Comparisons of Cornering and Ride Response Predictions with Linear Theory and with a Nonlinear Computer Simulation." CAL Report VJ-2251-V-5, May 1969.

9. C. V. Kroll and R. D. Roland, "A Preview-Predictor

Model of Driver Behavior in Emergency Situations." CAL Report VJ-2251-V-6, August 1970.

10. H. S. Radt and W. F. Milliken, "Motions of Skidding Automobiles." Paper 205A presented at SAE Summer Meeting, Chicago, June 1960.

11. R. R. McHenry and N. J. DeLeys, "Automobile Dynamics—A Computer Simulation of Three-Dimensional Motions for Use in Studies of Braking Systems and of the Driving Task." CAL Report VJ-2251-V-7, August 1970.

12. G. Newton, et al., U.S. Patent No. 2,354,219, July 25, 1944.

13. G. Krempel, "Research on Automobile Tires." Automobiltechnische Zeitschrift 69 (1969) 8.

14. Werner Gengenbach, "The Effect of Wet Pavement on the Performance of Automobile Tires." Universitat Karlsruhe, July 1967.

15. "Automotive Brakes." Chrysler Inst. of Engrg., Graduate School Lecture Notes, January 1952.

16. R. R. McHenry, "Analysis of the Dynamics of Automobile Braking." CAL Report VJ-2195-V-1, May 1966.

17. D. F. Kruse and R. C. Edwards, "Automobile Suspension Bumpers—A Correlation of Parameters Affecting Impact Response and a Technique for Achieving Effective Design." SAE Transactions, Vol. 77 (1968), paper 680471.

18. N. O. Tiffany, G. A. Cornell, and R. L. Code, "A Hybrid Simulation of Vehicle Dynamics and Subsystems." Paper 700155 presented at SAE Automotive Engineering Congress, Detroit, January 1970.

19. H. Strien, "Trends in the Development of Vehicle Brakes and Anti-Skid Braking Devices in Europe." Paper 304C presented at SAE Automotive Engineering Congress, Detroit, January 1961.

Society of Automotive Engineers, Inc.
TWO PENNSYLVANIA PLAZA, NEW YORK, N.Y. 10001

20 page booklet. Printed in U.S.A.